

Production and study of the stability of the ceramic compound $\text{Sr}_2\text{NiZrO}_6$ in crude petroleum for use as encapsulation for temperature sensors in the petroleum industry

Renata O. Domingues^{1*}, A. M. G. Soares¹, B. A. L. A. da Rocha¹,
Rebeka O. Domingues¹, B. S. Constantino², R. A. S. Ferreira¹, Y. P. Yadava¹

¹Universidade Federal de Pernambuco, PPGEM/CTG, 50740-550, Av. da Arquitetura, s/n, Recife, PE, Brazil

²Universidade Federal do Oeste da Bahia, Centro Multidisciplinar de Bom Jesus da Lapa, Bom Jesus da Lapa, BA, Brazil

Abstract

Ceramic compounds with complex cubic perovskite structures have shown to be promising materials for encapsulations for temperature sensors in the petroleum industry due to their high mechanical resistance and chemical inertness to the corrosive environment of crude oil. In this work, ceramic compounds were produced by solid-state calcination and the X-ray diffraction analysis verified the formation of the compound $\text{Sr}_2\text{NiZrO}_6$ with the ordered complex cubic perovskite structure of the $\text{A}_2\text{BB}'\text{O}_6$ type. The sintered $\text{Sr}_2\text{NiZrO}_6$ compound was characterized by scanning electron microscopy, energy dispersive X-ray spectroscopy, and Vickers microhardness. The chemical stability of the compound was verified through the structural, microstructural, and mechanical characterization of the specimens after 60 days of immersion in crude oil. The results showed that the compound did not present changes in the structure and did not suffer a chemical attack on its surface, thus presenting suitable properties for use as encapsulation for temperature sensors in oil wells.

Keywords: perovskite, stability in oil, ceramic temperature sensors.

INTRODUCTION

Petroleum is an important source of energy in the world. Even today, despite the emergence and development of new technologies that allow energy production from renewable sources, according to data presented by the International Energy Agency, its share in this consumption is quite significant in the world scenario, representing about 31% of the energy matrix [1]. In petroleum production, different types of sensors are used to monitor temperature, pressure, flow rate, and other important parameters. These sensors are subject to hostile operating conditions, such as high temperatures and aggressive action of crude oil, factors that can affect the accuracy of the results and reduce the lifespan of these devices. However, it is very important that these devices present stable and inert behavior under these working conditions [2]. In the oil industry, the type of temperature sensor commonly used is the so-called resistance temperature detectors (RTD), due to their high precision over a wide temperature range. Typically, these sensors are constructed with metals such as gold, platinum, and niobium as temperature-detecting elements encapsulated in inert ceramics [3]. Ceramic materials, although brittle and fragile, generally exhibit good chemical stability and hardness [4]. These characteristics are favorable for encapsulating temperature sensors in hostile environments such as crude oil.

In recent years, complex cubic perovskite ceramics

have been studied and considered as suitable materials for these purposes [5-8]. Complex perovskites with the formula $\text{A}_2\text{BB}'\text{O}_6$ are the result of the ordering of B and B' ions in the octahedral sites of the primitive perovskite unit cell [9], where A is a divalent alkaline earth cation, and B' and B'' are transition metals and present an octahedral coordination with the O^{2-} ions [10]. In this structure, both the cations in sites A and B can be replaced by different cations, A' and B', improving the structural stability of the perovskite and introducing structural and electronic defects [11]. Due to the increased complexity of the unit cell in these systems, it is possible to produce a wide variety of materials that exhibit a continuous progression of the lattice parameter. In this sense, this work aims to produce a complex cubic perovskite $\text{Sr}_2\text{NiZrO}_6$ from the nickelate series and study its chemical stability by analyzing its resistance to the corrosive environment of crude oil. Based on the study of the microstructural and mechanical characteristics of the new ceramic, its potential as encapsulation material in the manufacture of temperature sensors for petroleum wells is analyzed.

MATERIALS AND METHODS

For the production of $\text{Sr}_2\text{NiZrO}_6$, high-purity powders were used as raw materials: Sr_2CO_3 (99.9% purity, Sigma-Aldrich), ZrO_2 (99% purity, Sigma-Aldrich), and NiO (99.99% purity, Sigma-Aldrich). The compound was prepared by the conventional solid-state reaction route, in which the constituents were mixed in their stoichiometric amounts and homogenized using a high-energy ball mill for

*  <https://orcid.org/0009-0003-0738-9549>

24 h, compacted at 5 ton/cm² for 5 min, and calcined at 1250 °C for 24 h in an ambient atmosphere. After calcination, the samples were analyzed by X-ray diffraction technique to confirm the formation of the complex cubic perovskite structure. With the confirmation of the crystalline structure, the calcined samples were fragmented, homogenized again, and uniaxially compacted in a metal mold to form 15 mm diameter disks with approximately 4 mm thickness. For powder compaction, a hydraulic press was used in a hard steel mold (AISI A2 - HRC 58) and, to stabilize the pressure distribution in the pressed compact, the following pressing route was performed: load of 5 ton/cm² for 1 min, 7 ton/cm² for 1 min, and 10 ton/cm² for 3 min. Then, the samples were sintered in a muffle furnace (mod. 614, Jung) at 1350 °C for 24 h with a heating rate of 10 °C/min. The samples were cooled to room temperature without forced ventilation.

For the structural characterization of the ceramic compound, an X-ray diffractometer (XRD 700, Shimadzu) was used with CuK α radiation and wavelength $\lambda=1.5405$ Å, with a scanning angle of $10^\circ < 2\theta < 90^\circ$ and scanning speed of 1 °/min. The identification of peaks was made by qualitative analysis using the crystallographic files of the International Center for Diffraction Data (ICDD) database. The microstructure of the sintered ceramic was studied by scanning electron microscopy (SEM, Mira 3, Tescan) using 20 kV voltage and a backscattered electron (BSE) detector on the sample surface. The samples were covered with a 9 nm gold layer to allow electrical conduction to generate SEM images. To analyze the chemical composition of the sample, energy dispersive X-ray spectroscopy (EDS) was used through a detector coupled to the SEM capable of capturing X-rays and identifying the spectra of the constituent elements at a specific point of the sample. The mechanical behavior of the sintered ceramic compound was studied by the Vickers hardness test (HVS-5 21, Jenavert). The surface of the samples was previously polished with sandpapers of different granulometries until a mirrored surface was obtained. In order to obtain an average value of the hardness of the sample, 10 indentations were made in different regions of the polished sample, applying a load of 1000 g for 10 s using a diamond indenter with a square base pyramid shape. The Vickers microhardness (MHV) was calculated by:

$$\text{MHV}=1.8544F.d^{-2} \quad (\text{A})$$

where F is the applied load and d is the average diagonal of the pyramid base imprinted on the sample after indentation. The density and porosity of the Sr₂NiZrO₆ sintered ceramic were measured by the conventional Archimedes method. This method involved only measurements of the dry and saturated mass of the sample and followed the ABNT NBR 15845:2010 standard. After characterization, the sintered sample was submerged in crude oil. In order to verify its chemical and mechanical stability in the aggressive environment of the oil, after 60 days the sample was removed and a new structural, microstructural, and mechanical

characterization was performed.

RESULTS AND DISCUSSION

The X-ray diffraction (XRD) pattern of the powder calcined at 1250 °C is shown in Fig. 1. It is possible to observe the formation of the perovskite structure through the intense characteristic peaks of the primitive cubic structure of perovskite, as well as some weak reflection lines resulting from the superlattice reflections. The basic composition of perovskite (ABO₃) requires some prerequisites to ensure its stability: the element in the A site must be a cation with the largest ionic radius in the crystal structure, coordinated with 12 oxygen anions, forming a cubic close packing, while the element in the B site must be a cation with a smaller ionic radius than the A cation and coordinated with 6 oxygen anions so that the B element is inserted in octahedral spaces [9, 12]. When cations are substituted in simple perovskite, particularly in the B site, new multiple compounds of this unit are formed. They have larger unit cells, for example, A₂BB'O₆ and A₃B₂B'O₉, and are called complex perovskite [13]. Thus, in the composition of Sr₂NiZrO₆, Sr²⁺ with a larger ionic radius (1.26 Å) occupies the A site, while Ni²⁺ (ionic radius 0.69 Å) and Zr⁴⁺ (ionic radius 0.84 Å) occupy the B and B' sites in the B site due to their smaller ionic radii compared to Sr²⁺.

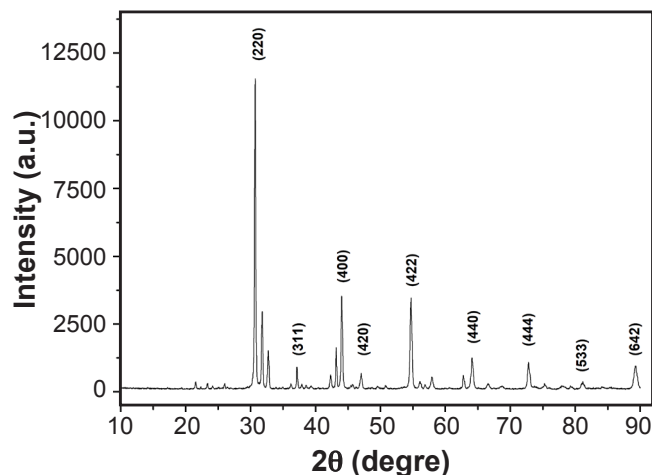


Figure 1: Powder X-ray diffraction pattern of Sr₂NiZrO₆ calcined at 1250 °C for 24 h.

Due to the ordering of B and B' in the octahedral site of the ABO₃ unit cell, there is a doubling in the lattice parameter of the basic unit cell of the cubic perovskite. Thus, the XRD pattern of the Sr₂NiZrO₆ compound was indexed in an A₂BB'O₆ cubic cell with the lattice parameter of the unit cell corresponding to twice the lattice parameter of the simple cubic perovskite ABO₃. The pattern obtained from the X-ray diffraction of the Sr₂NiZrO₆ ceramic is equivalent to those of complex cubic perovskite oxides of the A₂BB'O₆ type reported in the literature [14, 15], based on the comparison of d-spacing and peak intensity. The X-ray diffraction data of the Sr₂NiZrO₆ are presented in Table I. The presence of the

(311) and (533) reflection lines of the superstructure in the XRD pattern of the $\text{Sr}_2\text{NiZrO}_6$ ceramic compound confirmed the ordered complex cubic perovskite structure, where the Ni^{2+} and Zr^{4+} cations occupy the B and B' positions, as evidenced by the significant intensity of these superstructural reflection lines [16, 17]. The experimental lattice parameter of $\text{Sr}_2\text{NiZrO}_6$ calculated from the XRD experimental data is $a_{\text{exp}} = 8.2215 \text{ \AA}$. The theoretical lattice parameter calculation for materials with $\text{A}_2\text{BB}'\text{O}_6$ type structure is based on the rigid sphere approximation and was calculated using the following equations:

$$a_A = \frac{2(R_A + R_O)}{\sqrt{2}} \quad (\text{B})$$

$$a_B = R_B + R_{B'} + R_O \quad (\text{C})$$

$$a_{\text{calc}} = \frac{a_A + a_B}{2} \quad (\text{D})$$

where R_A , R_B , and $R_{B'}$ are the ionic radii of the cation A, B, and B', respectively, and R_O is the oxygen anion radius; a_A and a_B are the lattice parameters calculated based on the cations A and B, and a_{calc} is the average lattice parameter [14]. The theoretical lattice parameter calculated for the unit cell of $\text{Sr}_2\text{NiZrO}_6$ was $a_{\text{calc}} = 8.0918 \text{ \AA}$. The difference of about 1.60% between the theoretical and experimental lattice parameters of $\text{Sr}_2\text{NiZrO}_6$ was due to the rigid sphere approximation used in the calculation of the theoretical lattice parameter.

Table I: X-ray diffraction data of $\text{Sr}_2\text{NiZrO}_6$.

2θ	$d \text{ (\AA)}$	(hkl)	I/I_0
30.662°	2.913	(220)	1.000
37.195°	2.415	(311)	0.083
43.994°	2.057	(400)	0.309
47.033°	1.971	(420)	0.059
54.765°	1.675	(422)	0.300
64.097°	1.452	(440)	0.108
72.736°	1.299	(444)	0.096
81.134°	1.184	(533)	0.038
89.231°	1.097	(642)	0.084

The microstructural characteristics of ceramics play an important role in controlling crack propagation and energy dissipation mechanisms. In the production of ceramic compounds, it is important that the final product has low porosity and a uniform microstructure to avoid the creation of stresses that aid in the propagation of cracks and micro-fissures in the sintered body [15-18]. The microstructure of the sintered $\text{Sr}_2\text{NiZrO}_6$ ceramic at $1350 \text{ }^\circ\text{C}$ for 24 h, studied by scanning electron microscopy (SEM), is presented in Fig. 2. Through the micrographs, it was observed that the $\text{Sr}_2\text{NiZrO}_6$ presented a microstructure with uniform surface morphology, low porosity, and good homogeneity in grain size and distribution. In addition to SEM, energy dispersive

spectroscopy (EDS) was used for qualitative microanalysis of the chemical elements present in the sample. The darker points highlighted in the SEM images were identified as regions with a higher concentration of nickel. The confirmation of the presence of only the expected constituent elements Sr, Zr, Ni, and O can be seen in Fig. 3.

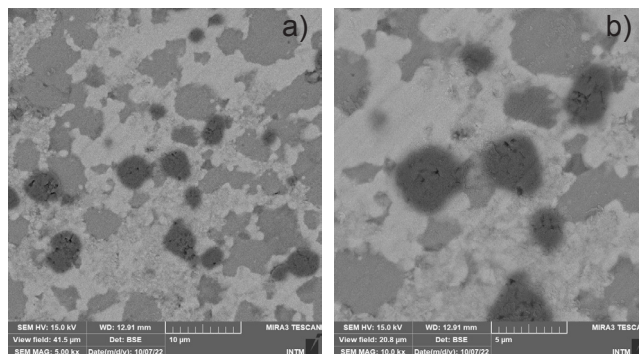


Figure 2: SEM micrographs of $\text{Sr}_2\text{NiZrO}_6$ ceramic sintered at $1350 \text{ }^\circ\text{C}$ at different magnifications.

The physical properties, density, and porosity, of the sintered $\text{Sr}_2\text{NiZrO}_6$ ceramic were obtained using the Archimedes method. These properties are important in characterizing ceramic compounds, as less porous materials tend to have better mechanical properties [19]. The calculated experimental value of the apparent density of $\text{Sr}_2\text{NiZrO}_6$ was 4.85 g/cm^3 and the porosity was 3.85%. These results showed that the sintered compound had reduced porosity. The mechanical properties of the new ceramic compound $\text{Sr}_2\text{NiZrO}_6$ sintered at $1350 \text{ }^\circ\text{C}$ were evaluated by Vickers hardness test. Different points on the polished surface of the ceramic were examined, resulting in an average microhardness value of $\text{MHV}=698 \text{ HV}$.

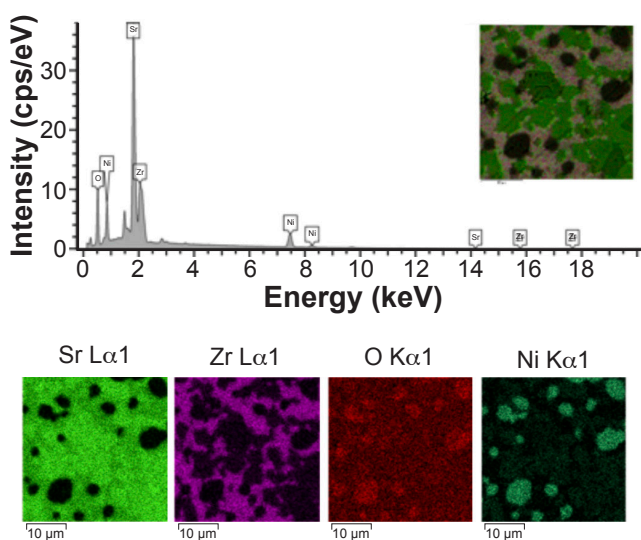


Figure 3: EDS spectrum (a) and elemental mapping for Sr (b), Zr (c), O (d), and Ni (e) of the sintered compound $\text{Sr}_2\text{NiZrO}_6$.

The chemical stability of the sintered ceramic was evaluated by immersion in crude oil from the Mossoró onshore exploration in Rio Grande do Norte State, Brazil. The previously characterized $\text{Sr}_2\text{NiZrO}_6$ samples were submerged in crude oil for 60 days, removed from the oil reservoir every 20 days, and evaluated to verify if there was any alteration in their structural, microstructural, and mechanical characteristics. The comparison between the X-ray diffraction patterns of the $\text{Sr}_2\text{NiZrO}_6$ ceramic before and after 60 days of immersion in crude oil is shown in Fig. 4. It is possible to observe that, despite the variation in peak intensities, the diffraction scan angles of the peaks remained unchanged, indicating that there was no alteration in the crystalline structure and no appearance of new phases. Additionally, in the XRD patterns of the $\text{Sr}_2\text{NiZrO}_6$ compound after immersion in crude oil, the characteristic (311) and (533) peaks of ordered complex perovskite oxides were also present.

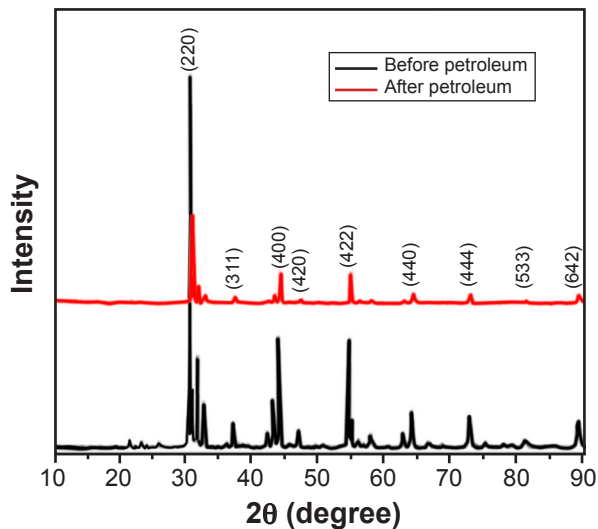


Figure 4: Comparison between X-ray diffraction patterns of $\text{Sr}_2\text{NiZrO}_6$ before and after 60 days of immersion in crude petroleum.

The microstructural analysis of $\text{Sr}_2\text{NiZrO}_6$ ceramics after immersion in crude petroleum was carried out using scanning electron microscopy. As shown in Fig. 5, it is possible to observe that there was no microstructural destructive effect on the samples or any other phenomenon that pointed to changes in the microstructural characteristics of the analyzed ceramics after contact with the oil. In the analysis of the mechanical characteristics, the average hardness value of the $\text{Sr}_2\text{NiZrO}_6$ ceramic compound after immersion in crude oil was $\text{MHV}=553$ HV, representing a reduction of approximately 21%. The difference between the average hardness values of the ceramic can be attributed to the superficial impregnation of crude oil on the sample, as hardness is measured by the surface penetration technique. This reduction did not interfere with the quality of the final product.

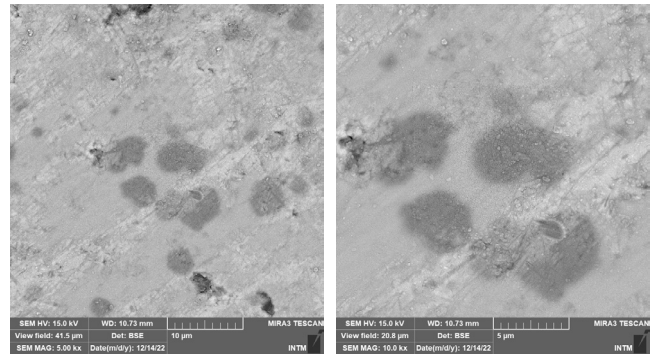


Figure 5: SEM micrographs of $\text{Sr}_2\text{NiZrO}_6$ sintered at 1350°C after immersion in crude petroleum for 60 days at different magnifications.

CONCLUSIONS

Ceramic compound $\text{Sr}_2\text{NiZrO}_6$, from the nickelate series, was produced by solid-state reaction. In the structural analysis, through the X-ray diffraction (XRD) pattern, the formation of the ordered complex cubic perovskite structure was confirmed, with an experimental lattice parameter of $a_{\text{exp}}=8.2215$ Å. The microstructural characteristics of the sintered ceramic were evaluated by scanning electron microscopy (SEM) and indicated a good homogeneity in the grain size and distribution. Through energy dispersive spectroscopy, the presence of only the constituent elements was verified, indicating that there was no contamination during the processing of the samples. The mechanical behavior of the ceramic compound sintered at 1350°C was studied by the Vickers hardness test, presenting an average hardness value of $\text{MHV}=698$ HV, which is sufficient for the encapsulation application of this ceramic. The physical properties of density and porosity, investigated through the Archimedes method, in which the calculated experimental apparent density value was 4.85 g/cm³ and the porosity was 3.85% revealed that the $\text{Sr}_2\text{NiZrO}_6$ ceramic had low apparent porosity. The stability of the sintered ceramic compound in crude oil was investigated through the structural, microstructural, and mechanical analysis of the sample after 60 days of immersion in crude oil. The results of XRD and SEM showed that the $\text{Sr}_2\text{NiZrO}_6$ ceramic submerged in crude oil did not undergo any changes at any stage of immersion. From these results, it can be concluded that $\text{Sr}_2\text{NiZrO}_6$ ceramics are inert to crude oil and are therefore considered potential candidates for ceramic encapsulation in the manufacture of temperature sensors for temperature monitoring in oil extraction wells.

ACKNOWLEDGMENT

The authors thank the National Council for Scientific and Technological Development - CNPq for the financial support for this research project.

REFERENCES

- [1] C.M. dos Santos, A.L.C. Braga, JM. dos Santos, M.B.

- Oliveira, M.T. Madureira, Res. Soc. Dev. **11**, 9 (2022) e40711932000.
- [2] F. Ropital, *Corrosion and degradation of metallic materials: understanding of the phenomena and applications in petroleum and processes industries*, Ed. Technips, Paris (2010).
- [3] J.C.S. Oliveira, R.A.S. Ferreira, Y.P. Yadava, in 57th Congr. Bras. Cerâm., Natal (2013).
- [4] W.D. Callister, *Ciência e engenharia de materiais: uma introdução*, LTC, S. Paulo (2002).
- [5] M.M. de Lima, R.O. Domingues, R.A.S. Ferreira, Y.P. Yadava, Mater. Res. **21**, 5 (2018) e20180139.
- [6] J.C.S. Oliveira, R.A.S. Ferreira, Y.P. Yadava, Mater. Sci. Forum **727-728** (2012) 731.
- [7] J.C.S. Oliveira, R.A.S. Ferreira, Y.P. Yadava, Mater. Sci. Forum **798-799** (2014) 154.
- [8] R.O. Domingues, Y.P. Yadava, R.A.S. Ferreira, Mater. Sci. Forum **820** (2015) 231.
- [9] V.J. Fratello, G.W. Berkstresser, C.D. Brandle, A.J. Van Graitis, J. Cryst. Growth **166** (1996) 878.
- [10] H.P.S. Corrêa, I.P. Cavalcante, D.O. Souza, E.Z. Santos, M.T.D. Orlando, H. Belich, F.J. Silva, E.F. Medeiro, J.M. Pires, J.L. Passamai, L.G. Martinez, J.L. Rossi, Cerâmica **56**, 338 (2010) 193.
- [11] M.C. Alves, S.O. Souza, J.C. Santos, M.J.B. Souza, A.M.G. Pedrosa, Cerâmica **57**, 343 (2011) 305.
- [12] X. Wang, B. Lu, H. Xia, Mater. Today Nano **21** (2023) 100291.
- [13] R. Roy, J. Am. Ceram. Soc. **37** (1954) 581.
- [14] V.J. Bradle, C.D. Fratelo, J. Mater. Res. **5**, 10 (1990) 2160.
- [15] B.S. Constantino, C.H. Gonzalez, N.L. Gomes, N.D.G. Silva, R.O. Domingues, R.A.S. Ferreira, Y.P. Yadava, J. Aust. Ceram. Soc. **57** (2021) 1425.
- [16] J. Koshy, J. Kurian, J.K. Thomas, Y.P. Yadava, A.D. Damodaran, Jpn. J. Appl. Phys. **33**, 1R (1994) 117.
- [17] J. Koshy, K.S. Kumar, J. Kurian, Y.P. Yadava, A.D. Damodaran, J. Am. Chem. Soc. **78**, 11 (1995) 3088.
- [18] P. Jha, A.K. Ganguli, Solid State Sci. **6**, 7 (2004) 663.
- [19] H.N. Yoshimura, A.L. Molisani, G.R. Siqueira, A.C. de Camargo, N.E. Narita, P.F. Cesar, H. Goldenstein, Cerâmica **51**, 319 (2005) 239.
- (Rec. 12/05/2023, Rev. 04/07/2023, Ac. 18/07/2023)

